Quantification of Local Reconstruction Accuracy for Helical CT with Motion Correction

Tao Sun, Rolf Clackdoyle, Roger Fulton, and Johan Nuyts

***Abstract*—In previous work, we have demonstrated the feasibility of rigid motion correction for helical CT brain imaging, using an optical motion tracking system. To correct for motion during reconstruction, the object is considered stationary, while the inverse of the motion is applied to the CT system. As a result, the original helical CT trajectory is replaced with a new, irregular trajectory. We have observed that, depending on the motion and the CT scanning parameters, the irregular motion corrected trajectory may not provide sufficient data for tomographic reconstruction. The known completeness conditions, such as the Tuy condition, assume untruncated projections and therefore can not be applied to helical CT, where the projections are axially truncated. Other groups have developed methods to quantify the degree to which sampling completeness is satisfied locally in pinhole SPECT. Here we propose a related approach to quantify the local completeness of the irregular CT trajectory, by assessing to which degree the local Tuy condition is unsatisfied. In a simulation experiment, we compare this empirical local completeness measure to the local occurrence of artifacts. The results indicate if the Tuy value is relatively high in some region, the reconstruction is likely to suffer from artifacts in this region.**

***Index Terms*—reconstruction, motion artifacts, projection completeness.**

I. Introduction

IN PET brain imaging, rigid motion correction can be obtained based on pose measurement using optical motion tracking [1], [2]. Previously we have applied a similar rigid motion correction technique to helical CT brain scans, by measuring the head motion with a Polaris system (Spectra, Northern Digital Inc., Waterloo, Canada) [3], [4]. We considered the patient head as stationary and applied the inverse of the motion to the helical CT. However, we found artifacts in certain regions of some reconstructed images after motion correction, in both simulation and phantom studies (Fig. 1). This may be due to the fact that the motion corrected projections are not complete for certain kinds of head motion, especially when the CT pitch is high (e.g. 1.5). Some methods to determine the sampling completeness in projections were introduced for pinhole SPECT [5], [6]. Another paper proposed a completeness map for a number of candidate cardiac CT system designs [7]. We have developed a similar method to quantify this incompleteness for motion corrected helical CT, as a predictor of the reconstruction accuracy. We have also verified the accuracy of this prediction with a phantom simulation.

Manuscript received May 11, 2014. This work was supported in part by the IWT MIRIAD SBO project.

T. Sun and J. Nuyts are with the Medical Imaging Research Center, Department of Nuclear Medicine, Katholieke Universiteit Leuven, Belgium.

R. Clackdoyle is with Laboratoire Hubert Curien, CNRS and Universit Jean Monnet, France.

R. Fulton is with the School of Physics, University of Sydney, and the Department of Medical Physics, Westmead Hospital, Westmead, Australia.

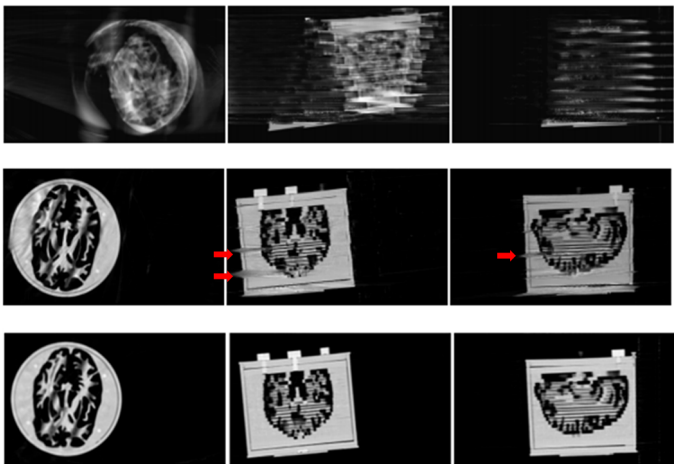

Fig. 1. Top: motion uncorrected image; Middle: motion corrected image; Bottom: reference image without motion. The CT scan was performed with a pitch of 1.0. [Window Level=-200HU, Window Width=+2000HU]

II. Method

A. Local Tuy condition

Firstly, a method to quantify local tomographic completeness based on the Tuy condition has been implemented. For non-truncated cone-beam projections, the Tuy condition states that the image can be reconstructed, if, for all voxels, every plane through the voxel contains at least one measurement line which passes through that voxel [8]. Since for motion-corrected helical CT the resulting cone-beam projections are often truncated, the Tuy condition will not hold anymore in our case. Meanwhile, Finch [9] proved the following converse of Tuy's result: if there is a plane passing through a particular voxel which contains no measurement lines, then stable reconstruction is not possible for this voxel. We can also view the Finch's argument as a local version of the Tuy condition.

Following [5], [6], we quantified the degree to which the Tuy condition is not satisfied in a voxel, and we call this measure the local Tuy value. For a particular voxel, all planes passing through that voxel are considered and, for each plane, we browse through all projection lines through the voxel. The plane is represented by a unit vector normal to that plane, the projection lines by unit vectors in the directions of the lines. The absolute value of the dot product of these vectors with the unit normal vector is computed, and the minimum

is stored for each plane. The local Tuy value for the voxel is then calculated as the maximum of those values across all planes. A higher value (ranges in [0, 1]) indicates that the local Tuy condition is violated more severely. A value of zero indicates that all planes through the voxel contain a projection line. Computing the voxel-based Tuy value can be divided into 3 steps in practice, which are explained in Algorithm 1.

Algorithm 1 Voxel-based Tuy value computation

1. Find all projection lines $\{\vec{l}\}$ passing through the voxel.
  for all projection angles/views **do**
    apply the inverse motion to projector
    calculate the source position O
    calculate the position of the detector corners $C1, C2, C3, C4$
    calculate the intersection point I on the detector
    if I is inside $C1C2C3C4$ **then**
      return $\vec{l} = \vec{OI}$
    end if
  end for
2. Find all norms $\{\vec{n}\}$ representing planes through the voxel, by uniformly sampling a unit sphere with center $(0, 0, 0)$.
  for all sampling points **do**
    get the sampling point coordinate S
    return $\vec{n} = S - (0, 0, 0)$
  end for
3. Compute Tuy value from worst plane.
  normalize the $\{\vec{l}\}$ and $\{\vec{n}\}$
  for all $\vec{n}$ in $\{\vec{n}\}$ **do**
    return $m_{\vec{n}} = \min_{\vec{l}} \left| \vec{l} \cdot \vec{n} \right|$
  end for
  return $localTuyvalue = \max_{\vec{n}} \{m_{\vec{n}}\}$

B. Phantom simulation

To demonstrate the potential projection incompleteness after motion correction and assess the predictive value of the local Tuy value, we need a phantom that reveals enough information. The Shepp-Logan phantom used in [3] contains large uniform regions, which might still be reconstructed correctly even when the data are incomplete. Therefore, we further designed a phantom with sufficient detail in all directions such that it could reveal reconstruction artifacts comprehensively. The phantom (image size $80 \times 80 \times 60$, voxel size $3 \times 3 \times 3$ mm^3) is shown in Fig. 2.

A 5 second motion recording of an awake rat [3] was applied to the phantom and a helical CT scan was simulated (Fig. 3). As was done in [3], all translations were multiplied by three, while the rotations were not modified, to produce motion values in a range that could be expected in a human scan.

The motion was then corrected for by incorporating its inverse in the projector and backprojector of an iterative reconstruction algorithm. The correction effectively replaces the (complete) helical trajectory with a new, irregular and possibly incomplete trajectory.

A Siemens Sensation 16 CT scanner (angles per rotation = 150, pitch = 1.5, collimation = 16×1.5 mm, energy = 70 kV) was simulated using IDL (Interactive Data Language). We applied the motion and performed a reconstruction using our motion correction scheme. We modified the Maximum Likelihood Transmission Reconstruction (MLTR) [10] algorithm to enable motion correction by allowing the pose of each projection to be individually specified in the scanner coordinate system. When motion was included, the detector and source were translated and rotated, and the (back)projection was computed using this displaced CT-system. This resulted in an arbitrary 3D motion of the virtual gantry around the patient head. In all reconstructions, 4 iterations and 60 subsets were used.

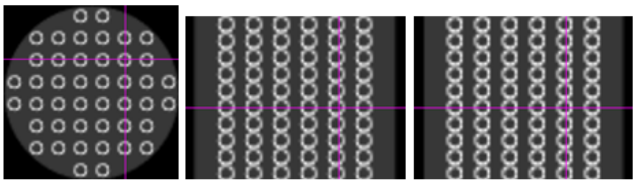

Fig. 2. Transaxial, coronal and sagittal view of the phantom in the field-of-view. Hollow spheres (inner diameter = 6 mm, outer diameter = 9 mm) were placed in the center on a rectangular grid of elements (size 15 mm x 15 mm) in the transverse plane, repeated for 10 transaxial slices (seperated by 9 mm). The foreground attenuation was set to 0.049 mm^{-1} (bone), while the background cylinder attenuation was set to 0.01 mm^{-1}.

C. Artifacts versus Tuy value

To quantify artifacts in the motion-corrected reconstruction image, we also performed a reconstruction of the phantom in section II.B without motion, to produce a reference image. The root mean square error (RMSE) between the two reconstructed images was then calculated, and compared with the Tuy value map obtained in II.A. We divided the images into small blocks, each being a $7 \times 7 \times 6$ neighborhood surrounding the center of each sphere. The similarity metric RMSE was then computed for all corresponding blocks. A similar sampling approach was applied to the Tuy value map. Therefore the final results were two vectors: one stores a metric value quantifying possible artifacts, and one stores the block-average Tuy value. A scatter plot was drawn to reveal the relationship between the local Tuy value and the artifact severity measure.

III. Results

The Tuy value map, which provided an indication of potential projection incompleteness within the reconstruction image space, is shown in Fig. 4. We found that slices 10 and 42 had the highest local Tuy values, indicating that these slices in the reconstruction may have severe artifacts. Visual assessment in Fig. 5, revealed a good correlation between the Tuy value map and the quality of the reconstruction. Fig. 6 and 7 confirmed this positive correlation quantitatively for all

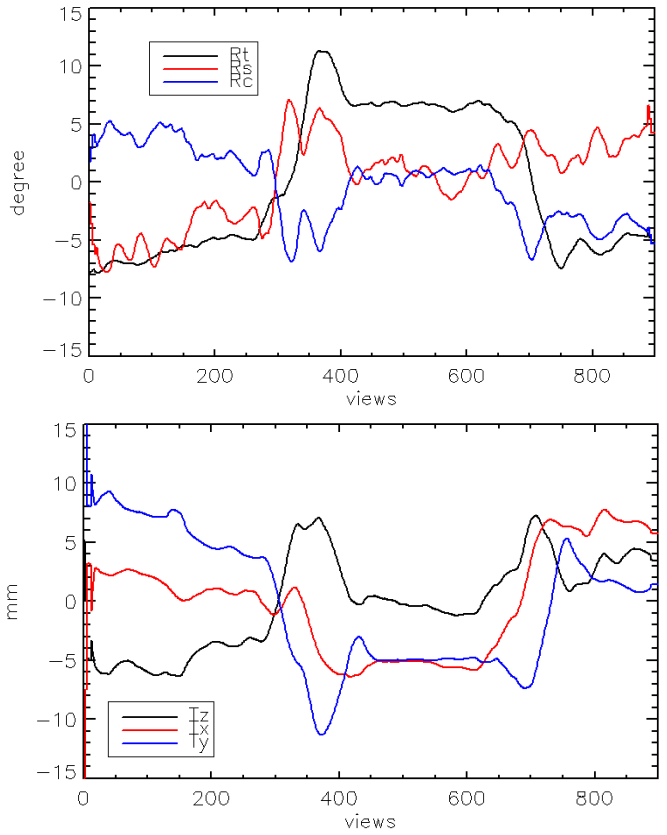

Fig. 3. Five-second rat motion. Upper: rotation, Rt is the rotation in transaxial plane, Rs is the rotation in sagittal plane, Rc is the rotation in the coronal plane; Lower: translation, Tx is the translation along x-axis, Ty is the translation along y-axis, Tz is the translation along z-axis.

the sampled blocks within the phantom.

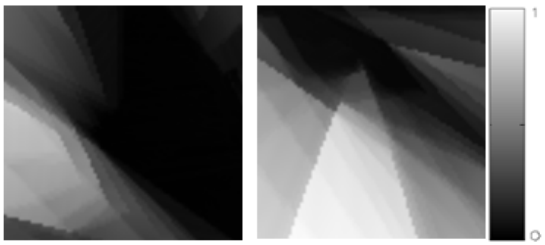

Fig. 4. Tuy value map when the rat motion was applied, left: slice 10 of 60, right: slice 42 of 60. White indicates high Tuy value and therefore poor tomographic sampling.

IV. Conclusion

An algorithm to quantify the local Tuy condition on a voxel-by-voxel basis within a motion correction scheme has been proposed. A first evaluation on simulations for a 16-slice CT scanner has been performed. The proposed Tuy value map provides a measure for the incompleteness in the projections, which may cause artifacts in the reconstructed images after motion correction. The preliminary results suggest that if

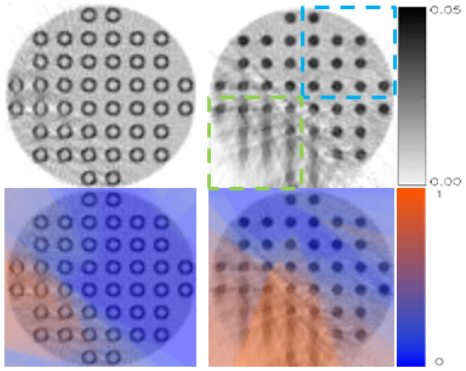

Fig. 5. Upper: image after MLTR with motion correction. Lower: the image overlayed with the corresponding Tuy value map. The green and blue dashed squares refer to Fig. 7.

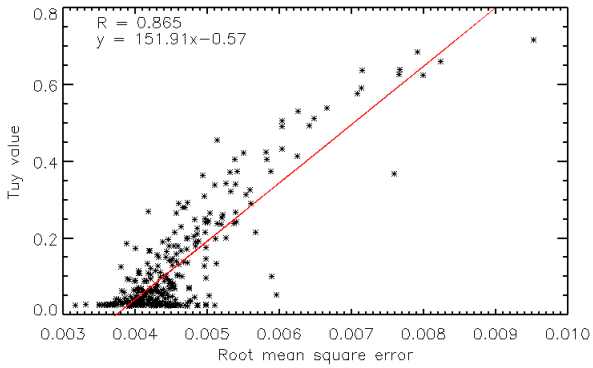

Fig. 6. The scatter plot shows the relationship between RMSE from reconstructed images and sampled Tuy value.

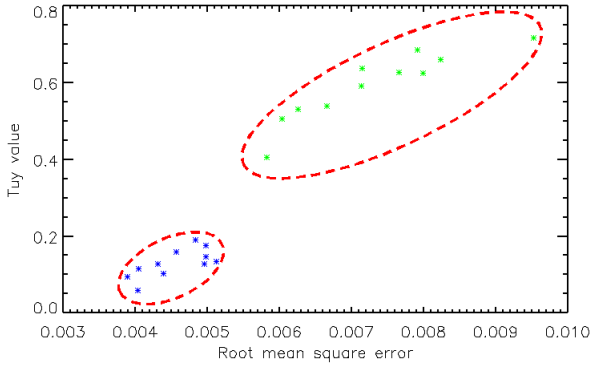

Fig. 7. The scatter plot shows the relationship between RMSE and Tuy value in certain regions in slice 42. Blue points correspond to samples in the blue region in Fig. 5, and the green points are to those in the green region.

the Tuy value is relatively high ($\sim$1) in some region, the reconstruction is likely to suffer from artifacts in this region. Also, for untruncated cone beam CT, it is known that exact reconstruction is possible if the Tuy value is zero everywhere. Our preliminary results suggest that this may also be true for cone beam CT with truncation, provided the Tuy value is zero everywhere.

ACKNOWLEDGMENT

The authors would like to thank Matthew Bickell for proof-reading.

REFERENCES

[1] A. Kyme, V. Zhou, S. Meikle, and R. Fulton, "Real-time 3D motion tracking for small animal brain PET." *Phys. Med. Biol.*, vol. 53, no. 10, pp. 2651–66, May 2008.

[2] A. Kyme, V. Zhou, S. Meikle, C. Baldock, and R. Fulton, "Optimised motion tracking for positron emission tomography studies of brain function in awake rats." *PLoS One*, vol. 6, no. 7, p. e21727, Jan. 2011.

[3] J. Nuyts, J.-H. Kim, and R. Fulton, "Iterative CT reconstruction with correction for known rigid motion," *11th Int. Meet. Fully 3D Reconstr. Radiol. Nucl. Med.*, pp. 132–135, 2011.

[4] J.-H. Kim, J. Nuyts, Z. Kuncic, and R. Fulton, "The feasibility of head motion tracking in helical CT: a step toward motion correction." *Med. Phys.*, vol. 40, no. 4, p. 041903, Apr. 2013.

[5] R. Clackdoyle and F. Noo, "Cone-beam tomography from 12 pinhole vertices," *2001 IEEE Nucl. Sci. Symp. Conf. Rec.*, vol. 4, pp. 1874–1876, 2001.

[6] S. Metzler, K. Greer, and R. Jaszczak, "Helical pinhole spect for small-animal imaging: a method for addressing sampling completeness," *IEEE Trans. Nucl. Sci.*, vol. 50, no. 5, pp. 1575–1583, Oct. 2003.

[7] B. Liu, J. Bennett, G. Wang, B. De Man, K. Zeng, Z. Yin, P. Fitzgerald, and H. Yu, "Completeness map evaluation demonstrated with candidate next-generation cardiac CT architectures." *Med. Phys.*, vol. 39, no. 5, pp. 2405–16, May 2012.

[8] H. K. Tuy, "An Inversion Formula for Cone-Beam Reconstruction," *SIAM J. Appl. Math.*, vol. 43, no. 3, pp. 546–552, 1983.

[9] D. V. Finch, "Cone Beam Reconstruction with Sources on a Curve," *SIAM J. Appl. Math.*, vol. 45, no. 4, pp. 665–673, Aug. 1985.

[10] J. Nuyts, B. De Man, P. Dupont, M. Defrise, P. Suetens, and L. Mortelmans, "Iterative reconstruction for helical CT: a simulation study." *Phys. Med. Biol.*, vol. 43, no. 4, pp. 729–37, Apr. 1998.